Electronic Supplementary Information to

Understanding CeO$_2$ as Deacon catalyst by probe molecule adsorption and in situ infrared characterisation

Ramzi Farra,[a] Sabine Wrabetz,[a] Manfred E. Schuster,[a] Eugen Stotz,[a] Neil G. Hamilton,[a] Amol P. Amrute,[b] Javier Pérez-Ramírez,[b] Núria López,[c] and Detre Teschner[a]

S.I.1   DFT calculations.

H   H OH   H Cl   Vac

(a) CeO$_2$ (b) CeO$_2$H   (c) CeO$_2$H-OH   (d) CeO$_2$H-Cl

NH$_3$

(e) CeO$_2$-NH$_3$ (f) CeO$_2$H-NH$_3$ (g) CeO$_2$H-OH-NH3   (h) CeO$_2$H-Cl-NH$_3$

CO$_2$

(i) CeO$_2$-CO$_2$ (j) CeO$_2$H-CO$_2$ (k) CeO$_2$H-OH-CO$_2$ (l) CeO$_2$H-Cl-CO$_2$ (m) CeO$_2$v-CO$_2$

CO

(n) CeO$_2$-CO   (o) CeO$_2$H-CO   (p) CeO$_2$H-OH-CO   (q) CeO$_2$H-Cl-CO

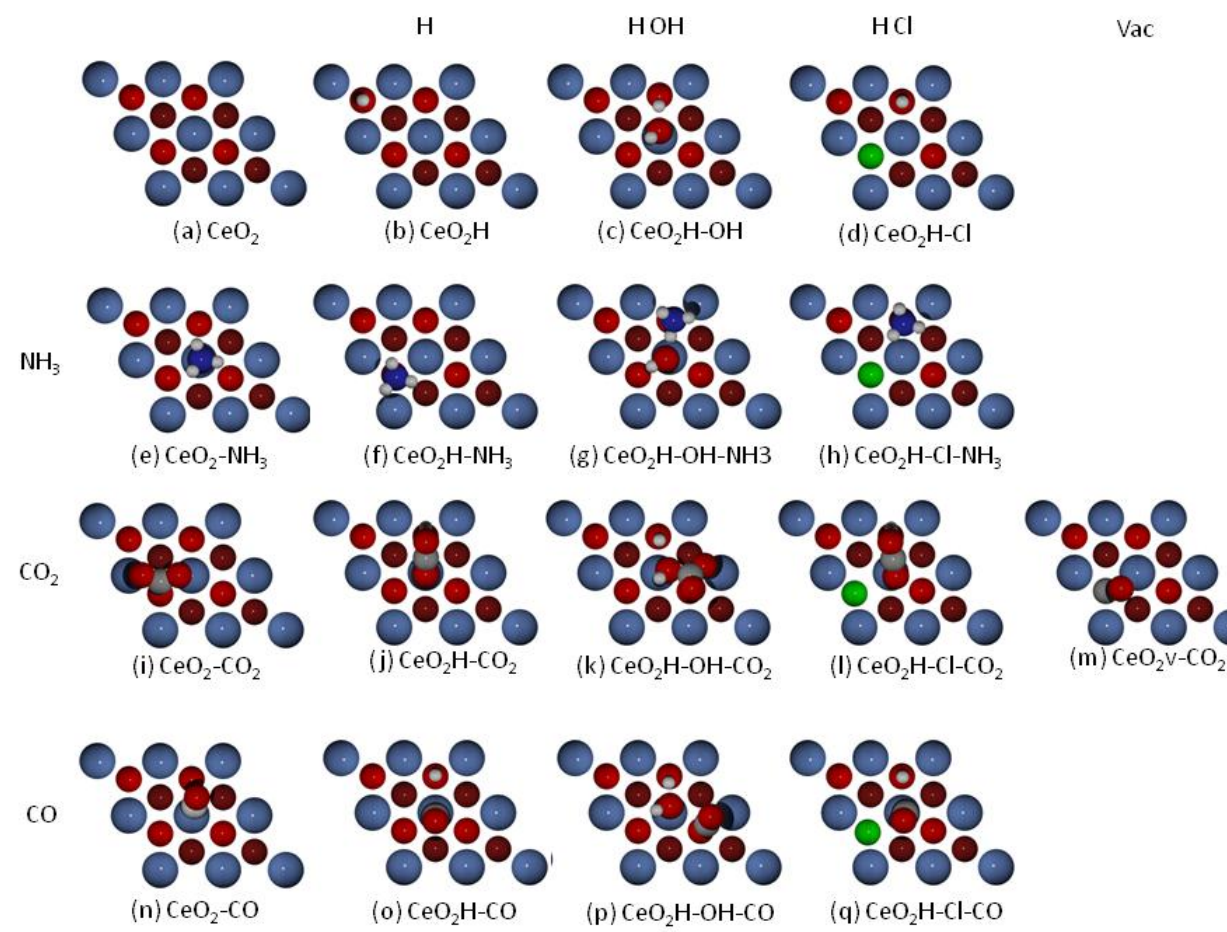**Figure S. I. 1.** Schematic representation of the clean CeO$_2$(111) surface (a), surface hydroxyl (b), surface on top hydroxyl (c) and chlorine substitution with a concomitant hydroxyl group (d). Ammonia adsorption on models (a-d) are represented in figures (e-h); CO$_2$ adsorption on figures (i-j) and adsorption on an oxygen vacancy (m) and CO adsorption on the (a-d) models shown in (n-q). Grey spheres represent Ce atoms, red O, blue H, yellow C and green Cl.

Table S. I. 1. Vibrational frequencies for hydroxyl groups on CeO_2, ν in cm^{-1}, for vibrations higher than 800 cm^{-1}. Frequency assignment labels: s: OH stretching; (b) bending modes. μ_B: Bohr magneton

	CeO_2H	CeO_2-OH_{top}	CeO_2-OH_{bridge}	CeO_2H-OH_{top}	CeO_2H-Cl
μ_B	0.5	1.0	1.0	0.0	2.0
1	3741 (s)	3714 (s)	3691 (s)	3786 (s)	3756 (s)
2				2953 (s)	
3				986 (b)	
4				890 (b)	

Table S. I. 2. Adsorption energies, E_{ads} in kJ mol^{-1}, of ammonia on different CeO_2 configurations (with respect to different model surfaces and gas-phase NH_3) and corresponding vibrational frequencies, ν in cm^{-1} (for the vibrations stronger than 800 cm^{-1}). Frequency assignment labels: symmetric stretching (ν_s), asymmetric stretching (ν_a), bending (δ modes). The labelling follows that of ref. [1] pages 117 and 131. μ_B: Bohr magneton

	Site	μ_B	Fig. S.I. 1	E_{ads} (kJ mol^{-1})	ν(cm^{-1})
Gas-phase NH_3	--	0.0		--	3509 (ν_a), 3506 (ν_a), 3370 (ν_s) 1627 δ_d (HNH), 1626 δ_d(HNH), 1021 δ_s(HNH)
Gas-phase NH_4^+	--	0.0		--	2873 (ν_a),2866(ν_a), 2862 (ν_a), 2812 (ν_s),1536 δ_d (HNH), 1532 δ_d (HNH), 1271 δ_d(HNH), 1265 δ_d (HNH), 1260 δ_d (HNH)
CeO_2	Ce N_{down}	0.0	(e)	50	3534 (ν_a), 3529 (ν_a), 3397 (ν_s), 1603 δ_d(HNH), 1593 δ_d(HNH), 1018 δ_s(HNH)
CeO_2	O_3 H_{down}	0.0		9	3690 (ν_a), 3550 (ν_a), 3290 (ν_s),1648 δ_d(HNH), 1582 δ_d(HNH)
CeO_2H	H N_{down}		(f)	39	3385 (ν_a), 3376 (ν_a), 3367 (ν_a), 1566 δ_d(HNH), 1562 δ_d(HNH), 997 δ_s(HNH), 948 δ_s(HNH)
CeO_2H-OH	H N_{down}	0.5	(g)	31	3662 (OH$_s$), 3552 (ν_a), 3476 (ν_a), 3119 (ν_s),2559 (HOH), 1632 δ_d(HNH), 1583 δ_d(HNH) 1145 δ_s(HNH), 1131δ_s(HNH), 1021δ_s(HNH)
CeO_2-H-Cl	H N_{down}	2.0	(h)	59	3513 (OH$_s$), 3510 (ν_a), 3393(ν_a), 2948 (ν_s), 1615 δ_d (HNH), 1612 δ_d (HNH), 1096 δ_s (HNH), 972 δ_s(HNH), 954 δ_s(HNH)
CeO_2-H	NH_4 at O	0.0		-113	3257 (ν_a), 3250 (ν_a), 3173 (ν_a), 2974 (ν_s), 1639 δ_d(HNH), 1637 δ_d(HNH), 1416 δ_d(HNH), 1408δ_d(HNH), 1340 δ_d(HNH)
CeO_2-H-Cl	NH_4 at Cl	0.0		-118	3583(ν_a), 3476(ν_a), 3271(ν_a), 2213 (ν_s), 1618 δ_d(HNH), 1611δ_d(HNH), 1415 δ_d(HNH), 1382 δ_d(HNH), 1274 δ_d(HNH)

Table S. I. 3. Adsorption energies, E_{ads} in kJ mol^{-1}, of CO_2 on different CeO_2 configurations and corresponding vibrational frequencies, ν in cm^{-1} (for the vibrations stronger than 800 cm^{-1}). Negative adsorption energies indicate endothermic processes. Frequency assignment labels: symmetric stretching (ν_s), asymmetric stretching (ν_a), bending (δ modes). The labelling follows that of ref. [1] page 108. *Multiple adsorption on oxygen vacancies leads to large binding energies linked to the position of the vacancy states, as those are poorly reproduced by PBE+U only a tentative assignment is presented. μ_B: Bohr magneton

	Site	μ_B	Fig. S.I. 1	E_{ads} (kJ mol^{-1})	ν (cm^{-1})
Gas-phase CO_2	--	0.0		--	2342 (ν_a), 1310 (ν_s)
Gas-phase CO_3^{2-}	--	0.0		--	1519 (ν_a), 1425(ν_a)
Gas-phase HCO_3^-	--	0.0		--	3511(OH), 1874 (ν_s)
CeO_2	O carbonate	0.0	(i)	43	1527 (ν_a), 1057 (ν_a), 829 ($\pi(CO_3)$)
CeO_{2-x}	Multiple adsorption (3)*	0.0	(m)	>120	--
CeO_{2-x}	Vacancy O-CO	0.0	(m)	14	1889(ν_a), 1105 (ν_s)
CeO_2H	Hydrocarbonate	1.0	(j)	-10	3720 (OH s), 2344 (ν_a), 1307 (ν_s)
CeO_2H-OH	Hydrocarbonate	0.0	(k)	18	3618 (OH s), 3588 (OH s), 1769(ν_s), 1242 (ν_s), 1132 (ν_s)
CeO_2H-Cl	Hydrocarbonate	2.0	(l)	1	3717 (OH s), 2247 (ν_a), 1252 (ν_s)

Table S. I. 4. Adsorption energies, E_{ads} in kJ mol^{-1}, of CO on different CeO_2 configurations and corresponding vibrational frequencies, n in cm^{-1} (for the vibrations stronger than 800 cm^{-1}). Negative adsorption energies indicate endothermic processes. Frequency assignment labels: stretching (s), bending (b). μ_B: Bohr magneton

	Site	μ_B	Fig. S.I. 1	E_{ads} (kJ mol^{-1})	ν (cm^{-1})
Gas-phase CO	--			--	2105 ($\square$)
CeO_2	Ce^{4+} C_{down}	0.0	(n)	18	2086 (s)
CeO_2H	Ce^{4+} C_{down}	0.5	(o)	12	3843 (OH s), 2127 (s)
CeO_2H-OH	O C_{down}	0.0	(p)	48	3781 (OHs), 2898 (OHs), 2113(s), 957(b), 881(b)
CeO_2H-Cl	Ce^{4+} C_{down}	2.0	(q)	23	3634 (OH s), 2157 (s)

S.I.2   Thermogravimetric profile of CeO$_2$-D and mass spectrometry analysis of effluent gases.
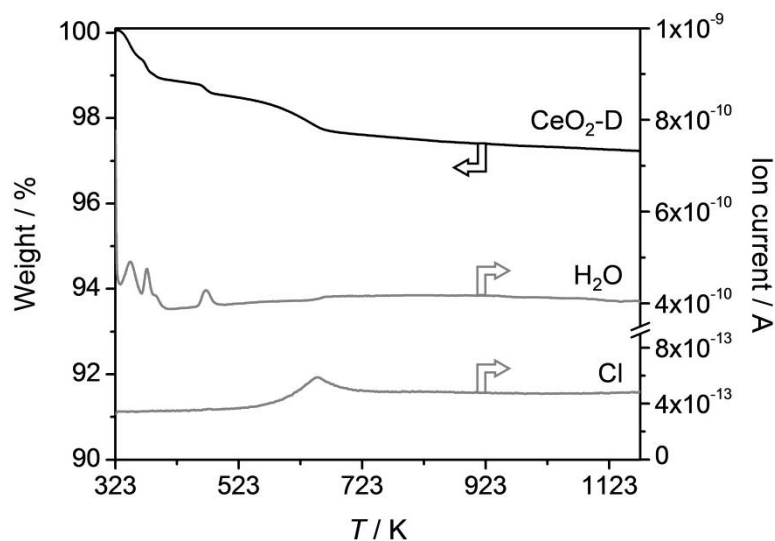

Fig. S. I. 2. Thermogravimetric (TGA) profile of CeO$_2$-D coupled to mass spectrometry (MS) profiles for H$_2$O (AMU 18) and for Cl (AMU 35). The weight loss of the equilibrated sample occurred in several steps. Up to 490 K, removal of surface impurities, such as physically adsorbed water, and the water of crystallisation of the CeCl$_3$·6H$_2$O phase took place. Weight loss between 490 and 660 K was attributed to chlorine removal. Similar assignments were made by Amrute *et al.* (*J. Catal.*, 2012, **286**, 287-297).

Procedure: Thermogravimetric analysis was performed in a Mettler Toledo TGA/DSC 1 Star system analyser connected to a Pfeiffer Vacuum ThermoStar GSD 320 T1 Gas Analysis System. Analyses were performed in He (20 cm^3 STP min^{-1}), ramping the temperature from 323 to 1273 K at 20 K min^{-1}. AMU 32 (O$_2$), 35 (Cl), 18 (H$_2$O), and 71 (Cl$_2$) were continuously monitored.

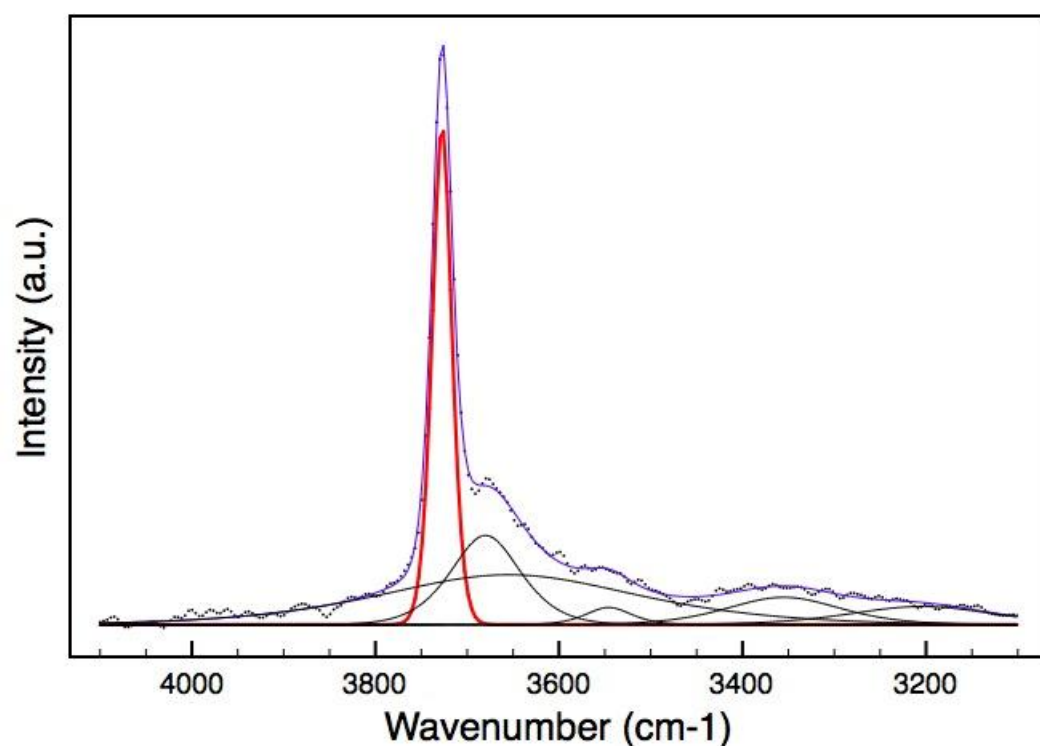S.I.3   Fit example of the OH region during *in situ* FTIR experiment.

Fig. S. I. 3. An example of fitting the OH region of *in situ* FTIR spectra observed during Deacon reaction. The red peak is integrated and discussed in the main text.

REFERENCES

[1] K. Nakamoto, Infrared and Raman spectra of inorganic and coordination compounds 4th Edition Wiley and Sons, New York 1986